Clinical Proteomics

RESEARCH

Open Access

Proteomic analysis of plasma exosomes in patients with metastatic colorectal cancer

Zhaoyue Zhong[1], Jiayin Ji[1], Hongxia Li[1], Ling Kang[1*] and Haipeng Zhu[2*]

Abstract

Background The diagnosis and treatment of colorectal cancer (CRC), especially metastatic colorectal cancer (mCRC), is a major priority and research challenge. We screened for expression differences in the plasma exosomal proteomes of patients with mCRC, those with CRC, and healthy controls (HCs) to discover potential biomarkers for mCRC.

Methods Plasma samples from five patients with mCRC, five patients with CRC, and five HCs were collected and processed to isolate exosomes by ultracentrifugation. Exosomal protein concentrations were determined using the BCA kit, and liquid chromatography-mass spectrometry was utilized to identify and analyze the proteins.

Results From the exosomes isolated from plasma samples, a total of 994 quantifiable proteins were detected, including 287 differentially expressed proteins identified by quantitative proteomics analyses. Totals of 965, 963 and 968 proteins were identified in mCRC patients, CRC patients, and HCs, respectively. The study identified 83 proteins with differential expression in the plasma exosomes of mCRC patients. The top 10 upregulated proteins in the mCRC group and CRC groups were ITGA4, GNAI1, SFTPA2, UGGT1, GRN, LBP, SMIM1, BMP1, HMGN5, and MFAP4, while the top 10 downregulated proteins were PSMB8, LCK, RAB35, PSMB4, CD81, CD63, GLIPR2, RAP1B, RAB30, and CES1. Western Blot validation data confirmed that ITGA4 and GNAI1 were unequivocally enriched in plasma-derived exosomes from mCRC patients.

Conclusions These differential proteins offer potential new candidate molecules for further research on the pathogenesis of mCRC and the identification of therapeutic targets. This study sheds light on the potential significance of plasma exosome proteomics studies in our understanding and treatment of mCRC.

Keywords Metastatic colorectal cancer, Neoplasm, Plasma exosomes, Proteomics

Introduction

Colorectal cancer (CRC) is globally recognized as the third most prevalent malignant tumor affecting the human digestive system. CRC is known to have an aggressive nature, with high morbidity and mortality rates, rapid metastasis, and resistance to treatment. mCRC, patients with colorectal cancer (CRC) and mortality rates, rapid metastasis,Colorectal cancer is now identified as the fourth leading cause of cancer-related deaths worldwide, and the incidence of new cases continues to rise annually [1]. Recent statistics from China revealed that the incidence rate of CRC is the second highest of all cancers, with 517, 100 new cases reported in 2022 [2]. The 5-year relative survival rates for different stages of CRC vary significantly, being 90% for localized disease, 72% for regional disease, and a mere 14% for distant metastatic CRC (mCRC) [3]. While early-stage CRC can be effectively treated through surgery and adjuvant radiotherapy and chemotherapy, mCRC remains incurable due

*Correspondence:
Ling Kang
lingkang1220@sina.com
Haipeng Zhu
834649852@qq.com
[1] School of Public Health, Xinjiang Medical University, No. 567, Shangde North Road, Shuimogou District, Urumqi 830017, Xinjiang, China
[2] Karamay Central Hospital, Number 67, Junggar Road, Karamay Region, Karamay 834000, Xinjiang, China

to the presence of treatment-resistant disseminated cancer cells [4]. Therefore, there is an urgent need to explore novel biomarkers and effective therapeutic targets for the better management of mCRC in patients.

Exosomes, a subtype of extracellular vesicles, are cell-derived nanovesicles containing various bioactive molecules, such as proteins, nucleic acids, lipids, and cytokines, and are found in a range of human body fluids. Recently, tumor-derived exosomes have emerged as promising sources of biomarkers [5, 6]. Traditional screening methods for CRC lack the necessary biological sensitivity and specificity for early cancer detection, and the invasiveness of colonoscopy often leads to poor patient compliance, resulting in late-stage diagnoses with unfavorable treatment outcomes and prognosis [7]. Tumor and tumor-associated macrophages interactions in the metastatic microenvironment, which are mediated by tumor-derived exosomes, affects CRC liver metastasis [8]. Regional disease, and 14% for distant metastatic colorectal.Therefore, it is urgent to discover novel biomarkers bioactive molecules including proteins, nucleic acids,

exosomal circLPAR1 has been shown to be internalized by CRC cells and suppress tumor growth [9]. These findings suggested that exosomal proteins play essential roles in the metastasis of CRC and can regulate tumor development [10]. Therefore, it is necessary that CRC researchers develop a deep understanding of the protein profiles of mCRC-derived exosomes.

Compared with other types of exosome cargo, proteins can provide abundant, stable, and distinct information about tumors [10].Network analysis combined with proteomics and phosphorylated proteomics data can be used to accurately predict drug responses and provide information important to the diagnosis and treatment of mCRC [11]. A study showed that disease-specific proteins on the surface of extracellular vesicles found in the plasma of patients with early-stage breast cancer offers potential candidates for the discovery of breast cancer biomarkers [12]. Studies of the non-small cell lung cance exosomal proteome have identified enriched proteins that may contribute to lung cancer progression and thus represent promising drug candidates [13]. Fu et al. found large amounts of exosomes containing SMAD3 in the peripheral blood of patients with hepatocellular carcinoma, and their levels correlated with disease stage and SMAD3 expression in the primary tumour [14]. The studies described above illustrate the importance of exosomal proteins in tumour research.

The survival of CRC patients relies heavily on their early diagnosis and treatment, emphasizing the necessity for reliable biomarkers. Studies on the non-small cell lung cancer (NSCLC) exosomal patients with Hepatocellular carcinoma (HCC), and their levels on early diagnosis and treatment, emphasizing the critical need for reliable biomarkers and asymptomatic patients in the early, treatable, stages of CRC with metastatic CRC (mCRC), offering we isolated exosomes from plasma samples. A total of 994 quantifiable proteins [15, 16]. This study employed a combination of proteomics and bioinformatics technologies to identify proteins associated with mCRC and obtain insights valuable to the diagnosis and treatment of mCRC. The growing body of research data and research suggests that numerous exosomal proteins play roles in the metastasis of CRC. It is hypothesized that plasma exosomal proteins can serve as valuable tools to identify potential biomarkers and therapeutic targets for mCRC. However, there is a lack of research on the proteomic profiles of plasma-derived exosomes from mCRC patients. The basis of this study was to obtain a comprehensive proteomic profile of exosomes from mCRC tissue by quantitative proteomics analysis and subsequently investigate the potential biological functions of these exosomal proteins using bioinformatics analysis. The aim was then to screen for differentially expressed proteins in the plasma exosomes of mCRC patients, uncover potential biomarkers of exosomal origin, and provide new strategies for diagnosis and treatment. The findings of this study are anticipated to serve as a valuable resource for further investigations in the field of mCRC.

Materials and methods

Patients and plasma samples

This study included five patients with mCRC, five patients with CRC, and five healthy individuals assessed at a tertiary hospital in Xinjiang between May 2023 and March 2024. The inclusion criteria required all participants with cancer to have a pathological diagnosis, with mCRC patients having stage IV disease and CRC patients having stage III disease. The patients had not undergone prior tumor-related radiotherapy or chemotherapy. The exclusion criteria were patients with other malignant tumors; other intestinal diseases; heart, liver, or kidney dysfunction; autoimmune diseases; blood diseases; or incomplete clinical data. Venous blood samples were collected from fasting participants, with 8–10 mL drawn and centrifuged at 3000×*g* in a high-capacity high-speed benchtop freezer centrifuge (CHT210R, China) for 10 min at 4 °C to obtain supernatant, which was stored at − 80 °C. The study received approval from the hospital ethics committee, and participants provided informed consent.

Isolation and extraction of plasma exosomes

Plasma samples were centrifuged at 4 ℃, 2000×*g* for 10min, and the supernatant was extracted and centrifuged at 4 ℃, 10,000×*g* for 30 min.The supernatant was extracted, and samples were transferred to

ultra-high-speed centrifuge tubes, centrifuged at 4 ℃, 110,000× for 75 min (Optiam™ L-90k Ultracentrifuge, Beckman Coulter), and the supernatant was discarded. The precipitates were resuspended in 1 mL 1 × PBS, and each of the precipitates was diluted with 1 × PBS after resuspension and filtered through a 0.22-μm-pore membrane. The samples were transferred to ultra-high-speed centrifuge tubes, centrifuged at 4 ℃, 110,000×*g* for 75 min and the supernatant discarded. The precipitate was resuspended in 1 × PBS and stored at − 80 °C.

Nanoparticle tracking analysis (NTA)

The size distribution of plasma exosomes was analyzed using a ZetaVIEW S/N 17-310 instrument (PARTICLE METRIX, Germany) equipped with nanoparticle tracking software (ZetaView 8. 04. 02). Frozen samples were thawed in a 25 °C water bath and placed on ice. Exosome samples were diluted in 1 × PBS for nanoparticle tracking analysis (NTA).

Transmission electron microscopy (TEM)

A 5 μL exosome sample was taken and applied to a copper grid, followed by a 5-min incubation at room temperature. After incubation, excess liquid was removed using absorbent paper. Subsequently, a drop of 2% hydrogen peroxide acetate was added to the copper grid and incubated at room temperature for 1 min. Again, excess liquid was removed using absorbent paper. The grid was then left to dry at room temperature for ~ 20 min before observation and imaging under a Tecnai G2 Spirit BioTwin electron microscope (FEI, USA).

Western blot analysis (WB)

To separate proteins based on molecular weight, a 1.5-mm glass plate and 15-well sample comb were used to create a separation gel and stacking gel. Electrophoresis was performed at a stable voltage of 80 V until the loading buffer entered the separation gel, then switched to 120 V until the loading buffer reached the bottom of the gel. The process was then terminated. For transfer, PVDF membranes with pore sizes of 0.22 μm and 0.45 μm were chosen, and a constant current of 200 mA was applied for 90 min. Blocking was achieved by adding 5% skim milk powder diluted in PBST, followed by 1-h blocking and a 30-min wash with PBST. The membrane was then incubated with primary antibodies, namely anti-CD9 antibody (EXOAB-CD9A-1; SBI, USA; 1:1,000), anti-CD81 antibody (YT5394; Immunoway, USA; 1:500), anti-TSG101 antibody (EXOAB-TSG101-1; SBI; 1:1000), anti-calnexin antibody (Immunoway), anti-integrin alpha 4 antibody (AB81280; Abcam, UK; 1:2000), and anti-GNAI1 antibody (AB140125; Abcam; 1:8000). After overnight incubation at 4 °C, the membrane was incubated with exosome-validated HRP-conjugated goat anti-rabbit secondary antibody (180202-001; SBI; 1:20,000). Following washing steps with PBST, ECL luminescent solution was added, and imaging was performed using a Tanon 5200 fully automatic chemiluminescence image analysis system (Tanon, Shanghai, China).

Exosome protein extraction and sample preparation

A specified volume of exosome suspension in PBS was combined with an equal volume of RIPA lysis buffer for protein extraction. The mixture was shaken and lysed at 4 °C for 30 min, with periodic shaking every 10 min. Following this, the lysate was centrifuged at 13,200 rpm at 4 °C for 15 min, and the supernatant was transferred to a new tube for protein quantification using the BCA protein assay reagent kit (Beyotime, China). After determining the protein concentration, 50 μg of protein solution was removed, and the lysate volume adjusted accordingly. Dithiothreitol (DTT) was added to achieve a final concentration of 10 mM, and the solution was mixed and incubated at 37 °C for 1 h. Indole acetic acid (IAA) was then added at a volume ratio of DTT:IAA = 1:5, thoroughly mixed, and incubated in the dark for 40 min. Subsequently, the solution was precipitated with five times the volume of precipitation reagent for 1 h, followed by centrifugation at 13,000 rpm, 4 °C for 1 h, and removal of the supernatant. The precipitate was washed with 1 mL of 100% acetone, centrifuged at 13,000 rpm for 30 min, and the process was repeated. The dried precipitate was then subjected to trypsin digestion overnight at 37 °C. The resulting peptides were concentrated by centrifugation, desalted using a Monospin column, and dried prior to mass spectrometry analysis. The dried mixed peptides were dissolved in 0.1% trifluoroacetic acid (TFA) solution. The desalting column was activated with 100% acetonitrile and balanced with 0.1% TFA solution. The sample was added to the desalting column, centrifuged, washed with 0.1% TFA solution, and eluted with 50% acetonitrile solution. The eluted solution was collected in a new tube, centrifuged, concentrated, and dried to remove the acetonitrile.

Liquid chromatography–mass spectrometry (LC–MS) analysis

LC–MS analysis was conducted using a nanoflow UPLC system (Brucker, Germany), specifically the Brucker NanoElute, for chromatographic separation. The buffers consisted of a 0.1% formic acid aqueous solution for solution A and a 0.1% formic acid acetonitrile solution for solution B. Prior to loading the sample, the column was equilibrated with 100% solution A. The sample was then loaded onto an analytical column (Aurora UPLC Column, C18 1.6 μm, 250 mm × 75 μm) using an automatic injector

for separation with a flow rate of 300 nL/min. The liquid phase separation gradient proceeded as follows: from 0 to 45 min, there was a linear gradient of 2% to 22% liquid B; from 45 to 50 min, the gradient was increased from 22 to 35%; from 50 to 55 min, it was further increased from 35 to 80%; and from 55 to 60 min, the gradient was maintained at 80% liquid B. The samples separated by nanoliter high-performance liquid chromatography were then analyzed using DDA mass spectrometry with a timsTOF Pro mass spectrometer (Brucker). The analysis lasted 60 min, and the detection mode employed was positive ion. The first level mass spectrometry scan range was utilized, with 100–1700 m/z, 1/K0 start: 0.75 Vs/cm^2, 1/K0 end: 1.40 Vs/cm2; intensity threshold: 5000.00; absolute threshold: 10; target intensity: 10,000 cts/s; release after: 0.50 min; no. of PASEF MS/MS scans: 10.

Bioinformatics analysis

Proteins were analyzed for significant differences in expression. Then, the clustering of differential proteins, Gene Ontology (GO, https://www.geneontology.org/) enrichment, Kyoto Encyclopedia of Genes and Genomes (KEGG, https://www.kegg.jp/kegg/pathway.html) pathway enrichment, and protein–protein interaction networks (PPI network, STRING database, https://string-db.org/) were analyzed.

Statistical analysis

When comparing two groups, the mean value of all sample signals within each group was calculated to ascertain the fold-change in intergroup ratio, and the p-value of the difference between the two groups was calculated using Student's t test. Proteins that met the following two conditions were assigned as being differentially expressed between groups: (1) a fold-change in intergroup ratio ≥ 1.2 or $\leq 1/1.2$; (2) a p-value < 0.05. The exosomal ITGA4 and GNAI1 levels in mCRC patients, CRC patients, and healthy controls were compared using a one-way analysis of variance using GraphPad Prism 7 software. A two-sided $p < 0.05$ was defined as indicating a statistically significant difference.

Results

Isolation and identification of exosomes

Exosomes from combined plasma samples from mCRC patients, CRC patients, and healthy controls were isolated by ultracentrifugation and analyzed by transmission electron microscopy (TEM), NTA, and western blotting (WB). The morphological analysis using TEM showed the exosomes were cup-shaped or rounded, consistent with typical exosome structures (Fig. 1A). NTA showed an average purified exosome size of 111.5 ± 49. 4 nm, with the main peak size being 98.7 nm, and a concentration of approximately 1.4 × 1011 particles/mL (Fig. 1B). In addition, WB showed the significant expression of exosome marker proteins (CD9, CD81, and TSG101) and an absence of calreticulin (Fig. 1C) in the exosome samples. These results indicated exosomes were successfully isolated from clinical plasma samples.

Proteomic analysis of exosomes

In this study, a total of 994 plasma exosome proteins were identified by label-free quantitative proteomic analysis. In total, 965 and 963 proteins were identified in mCRC patients and CRC patients, respectively (Fig. 2A). A total of 83 differentially expressed proteins were identified in the mCRC and CRC groups by quantitative protein analysis, of which 36 were upregulated and 47 were downregulated (Fig. 2B, C). Hierarchical cluster analyses were performed on the mCRC and CRC groups' proteomics data, and heat maps were generated (Fig. 2D). Tables 1 and 2 list the top 10 up- and downregulated plasma exosomal differentially expressed proteins in the mCRC group and CRC group, respectively.

GO function enrichment analysis

GO function enrichment analysis was performed on the screened differential proteins. The mCRC GO results were divided into three main categories: biological process, cellular component, and molecular function. Biological processes mainly included blood coagulation, cell activation, cell–matrix adhesion, coagulation, hemostasis, homotypic cell–cell adhesion, platelet activation, platelet aggregation, regulation of body fluid levels, and response to wounding. The cellular components mainly included extracellular exosome, extracellular membrane-bound organelle, extracellular region, extracellular space, extracellular vesicle, secretory granules, secretory vesicles, vesicles, and vesicle lumen. Molecular functions mainly included carbohydrate derivative binding, cell adhesion molecule binding, extracellular matrix structural constituent, GTPase activity, hydrolase activity, acting on acid anhydrides, integrin binding, protein-containing complex binding, pyrophosphatase activity, ribonucleoside triphosphatase phosphatase activity, and signaling receptor binding (Fig. 3).

KEGG pathway enrichment analysis

The screened differential proteins were subjected to KEGG pathway analysis and found to be mainly concentrated within the proteasome, pyruvate metabolism, malaria, platelet activation, ECM-receptor interactions, glycolysis/gluconeogenesis, circadian entrainment, focal adhesion, phagosome, leukocyte transendothelial migration, Rapl signaling pathway, human cytomegalovirus infection, chemokine signaling pathway, PI3K-Akt

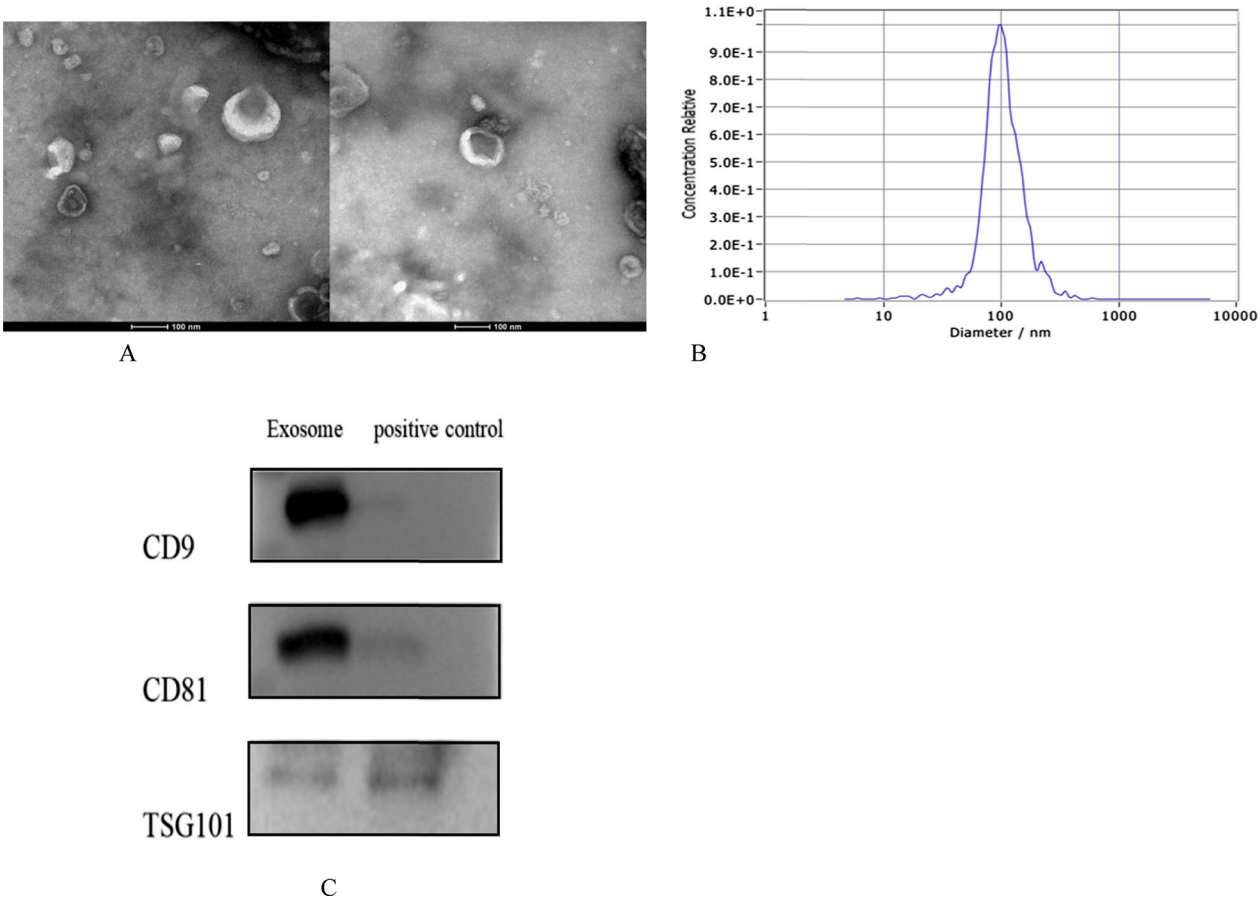

Fig. 1 Isolation and characterization of plasma exosomes. **A** Transmission electron microscopy (TEM) image of plasma exosomes. **B** Nanoparticle tracking analysis (NTA) of plasma exosomes. **C** Western blot analysis of exosome protein markers (CD9, CD81, TSG101)

signaling pathway, and human papillomavirus infection categories (Fig. 4).

PPI interaction network analysis

The differential proteins were subjected to PPI network analysis, and it was found that five clusters of differential proteins might have direct or indirect interactions (Fig. 5A). To ascertain the key molecules within the relationship networks of the differential proteins, 10 proteins with the highest degree of connectivity were screened out. These were ITGA4, CD81, CD9, ITGB3, FGA, FGG, THBS1, ITGA2B, RAP1A, and RAP1B (Fig. 5B). The findings indicated there were enhanced biological connections, among these proteins, but further validation of their biological functions is needed.

Validation of ITGA4 and GNAI1 proteins using western blot analysis

Based on the results of the bioinformatics analysis, ITGA4 and GNAI1 were selected to validate the proteomics results. We re-collected samples from the 30 cases, isolated the exosomes by ultracentrifugation, and then verified their protein profiles with WB. The expression levels of ITGA4 and GNAI1 in plasma exosomes were detected by WB.β-ACTIN was used as the internal control, as it is a standard marker of exosomes. As shown in Fig. 6A–F the expression levels of exosomal ITGA4 and GNAI1 were significantly higher in mCRC patients than in CRC patients and healthy controls, which is consistent with our proteomics results.

Discussion

Exosomes are released by various cell types, including tumor cells, and are crucial in intercellular communication, signaling, and waste metabolism. In the context of tumor growth and metastasis, exosomes regulate immune responses, inhibit epithelial–mesenchymal transition, promote angiogenesis, and contribute to chemotherapy resistance [17]. These small vesicles have diverse extracellular functions in tumor development, including their transfer to recipient cells, and are recognized as key components of the tumor microenvironment

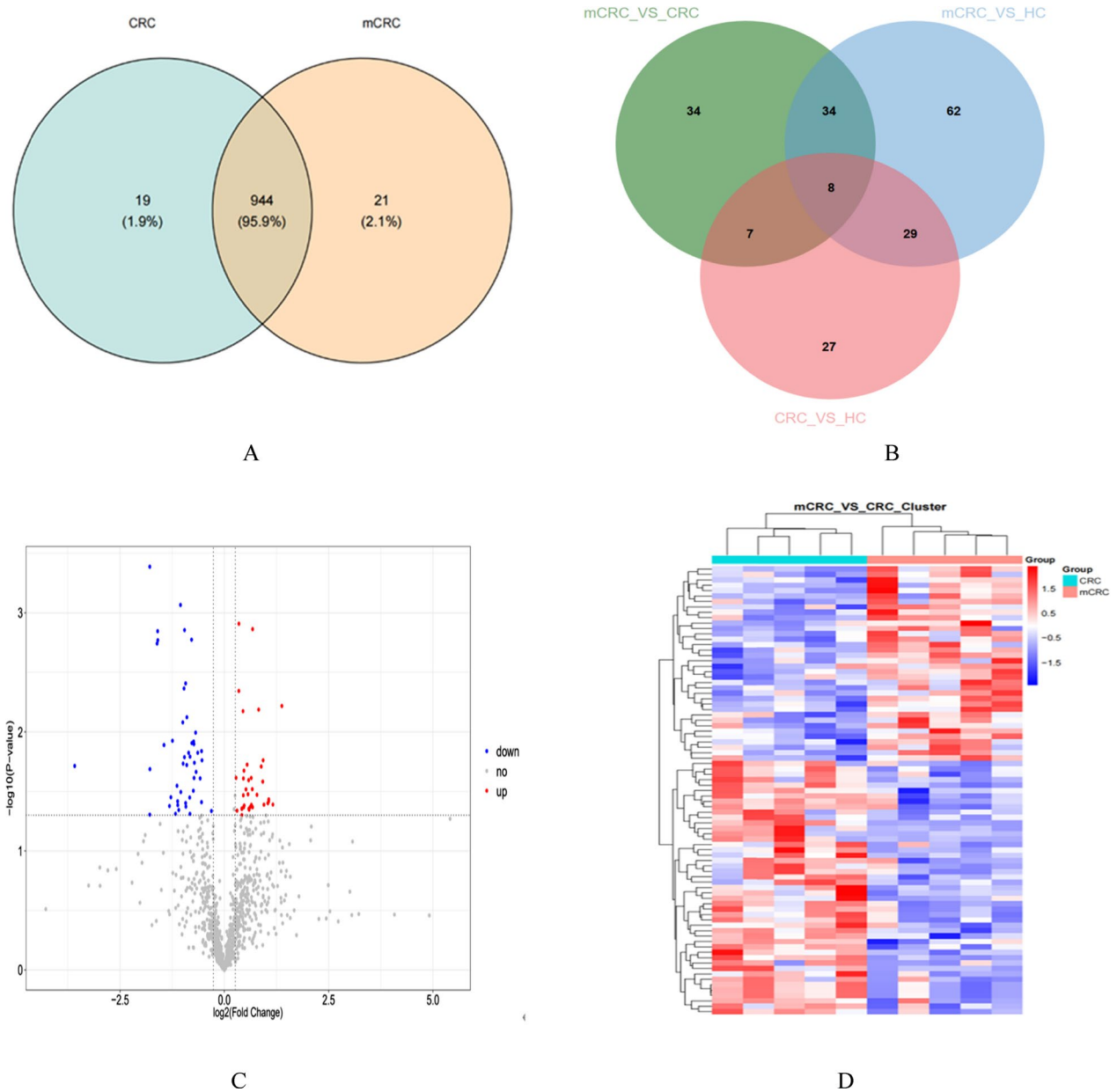

Fig. 2 Proteomic analysis of mCRC exosomes. **A** Venn diagram displaying the expression of exosomal proteins in mCRC and CRC patients. **B** Venn diagram showing the expression of differential exosomal proteins in two-by-two comparisons of the three groups: mCRC patients, CRC patients, and healthy controls (HC). **C** Volcano plot of differences in protein quantification results between the mCRC and CRC groups. **D** Heatmap of differentially expressed protein clustering in the mCRC and CRC groups

[18, 19]. Ongoing research is delving into the multifaceted roles of exosomes in health and disease, with a focus on their clinical applications. While progress has been made in utilizing exosomes for tumor diagnosis and treatment, the field is still evolving. Early investigations in rectal cancer leveraged high-sensitivity genomic sequencing techniques and liquid biopsies to gain deeper insights into the genetic landscape of mCRC, as well as to unravel the molecular evolution and mechanisms of treatment resistance [20]. A comprehensive proteomic analysis of extracellular vesicles and particles (EVPs) from 426 human samples identified pan-EVP markers that represent biomarkers for EVP isolation, cancer detection, and the identification of cancer types [21].

The upregulated exosomal circATG4B derived from oxaliplatin-resistant CRC cells can be transferred to

Table 1 Differential expression of top 10 upregulated proteins in the mCRC and CRC groups

No.	Accession	GeneSymbol	Description	mCRC/CRC ratio	P-value
1	P13612	ITGA4	Integrin alpha-4 OS = Homo sapiens OX = 9606 GN = ITGA4 PE = 1 SV = 3	2.603	0.006
2	P63096	GNAI1	Guanine nucleotide-binding protein G(i) subunit alpha-1 OS = Homo sapiens OX = 9606 GN = GNAI1 PE = 1 SV = 2	2.241	0.041
3	Q8IWL1	SFTPA2	Pulmonary surfactant-associated protein A2 OS = Homo sapiens OX = 9606 GN = SFTPA2 PE = 1 SV = 2	2.087	0.037
4	Q9NYU2	UGGT1	UDP-glucose:glycoprotein glucosyltransferase 1 OS = Homo sapiens OX = 9606 GN = UGGT1 PE = 1 SV = 3	2.083	0.038
5	P28799	GRN	Progranulin OS = Homo sapiens OX = 9606 GN = GRN PE = 1 SV = 2	2.058	0.040
6	P18428	LBP	Lipopolysaccharide-binding protein OS = Homo sapiens OX = 9606 GN = LBP PE = 1 SV = 3	1.928	0.041
7	B2RUZ4	SMIM1	Small integral membrane protein 1 OS = Homo sapiens OX = 9606 GN = SMIM1 PE = 1 SV = 1	1.902	0.017
8	P13497	BMP1	Bone morphogenetic protein 1 OS = Homo sapiens OX = 9606 GN = BMP1 PE = 1 SV = 2	1.891	0.026
9	P82970	HMGN5	High mobility group nucleosome-binding domain-containing protein 5 OS = Homo sapiens OX = 9606 GN = HMGN5 PE = 1 SV = 1	1.843	0.020
10	P55083	MFAP4	Microfibril-associated glycoprotein 4 OS = Homo sapiens OX = 9606 GN = MFAP4 PE = 1 SV = 2	1.767	0.007

Table 2 Differential expression of top 10 downregulated proteins in the mCRC and CRC groups

No.	Accession	GeneSymbol	Description	mCRC/CRC ratio	P-value
1	P28062	PSMB8	Proteasome subunit beta type-8 OS = Homo sapiens OX = 9606 GN = PSMB8 PE = 1 SV = 3	0.806	0.046
2	P06239	LCK	Tyrosine-protein kinase Lck OS = Homo sapiens OX = 9606 GN = LCK PE = 1 SV = 6	0.690	0.017
3	Q15286	RAB35	Ras-related protein Rab-35 OS = Homo sapiens OX = 9606 GN = RAB35 PE = 1 SV = 1	0.685	0.014
4	P28070	PSMB4	Proteasome subunit beta type-4 OS = Homo sapiens OX = 9606 GN = PSMB4 PE = 1 SV = 4	0.685	0.039
5	P60033	CD81	CD81 antigen OS = Homo sapiens OX = 9606 GN = CD81 PE = 1 SV = 1	0.669	0.025
6	P08962	CD63	CD63 antigen OS = Homo sapiens OX = 9606 GN = CD63 PE = 1 SV = 2	0.643	0.015
7	Q9H4G4	GLIPR2	Golgi-associated plant pathogenesis-related protein 1 OS = Homo sapiens OX = 9606 GN = GLIPR2 PE = 1 SV = 3	0.625	0.022
8	P61224	RAP1B	Ras-related protein Rap-1b OS = Homo sapiens OX = 9606 GN = RAP1B PE = 1 SV = 1	0.620	0.010
9	Q15771	RAB30	Ras-related protein Rab-30 OS = Homo sapiens OX = 9606 GN = RAB30 PE = 1 SV = 2	0.608	0.018
10	P23141	CES1	Liver carboxylesterase 1 OS = Homo sapiens OX = 9606 GN = CES1 PE = 1 SV = 2	0.605	0.024

recipient cells, where it induces oxaliplatin resistance. The recently identified circATG4B-222aa is a vital biomarker and potential therapeutic target in oxaliplatin-resistant CRC [22]. The expression levels of exosomal miR-139-3p are decreased in CRC patient plasma and may act as a novel biomarker for the early diagnosis and metastasis monitoring in CRC [23].

In this study, plasma samples were collected from patients with mCRC and CRC and healthy controls for plasma exosome proteomic analysis. Exosomes were characterized using TEM, NTA, and WB. A comprehensive proteomic analysis of these exosomes was conducted using LC–MS, a technology known for its high sensitivity, selectivity, accuracy, and throughput in limited sample proteomics [24]. A total of 994 exosome proteins, including 287 differentially expressed proteins, were identified by quantitative proteomics analyses, with 83 proteins (36 upregulated and 47 downregulated) showing differential expression in plasma exosomes from mCRC patients. The functionally classified differentially expressed proteins were found to be involved in various processes, such as blood coagulation, cell activation, cell–matrix adhesion, extracellular vesicle, and cell adhesion molecule binding, highlighting their role in intercellular communication. The top 10 upregulated proteins in the mCRC and CRC groups were ITGA4, GNAI1, SFTPA2, UGGT1, GRN, LBP, SMIM1, BMP1, HMGN5, and MFAP4, while the top 10 downregulated proteins were PSMB8, LCK,

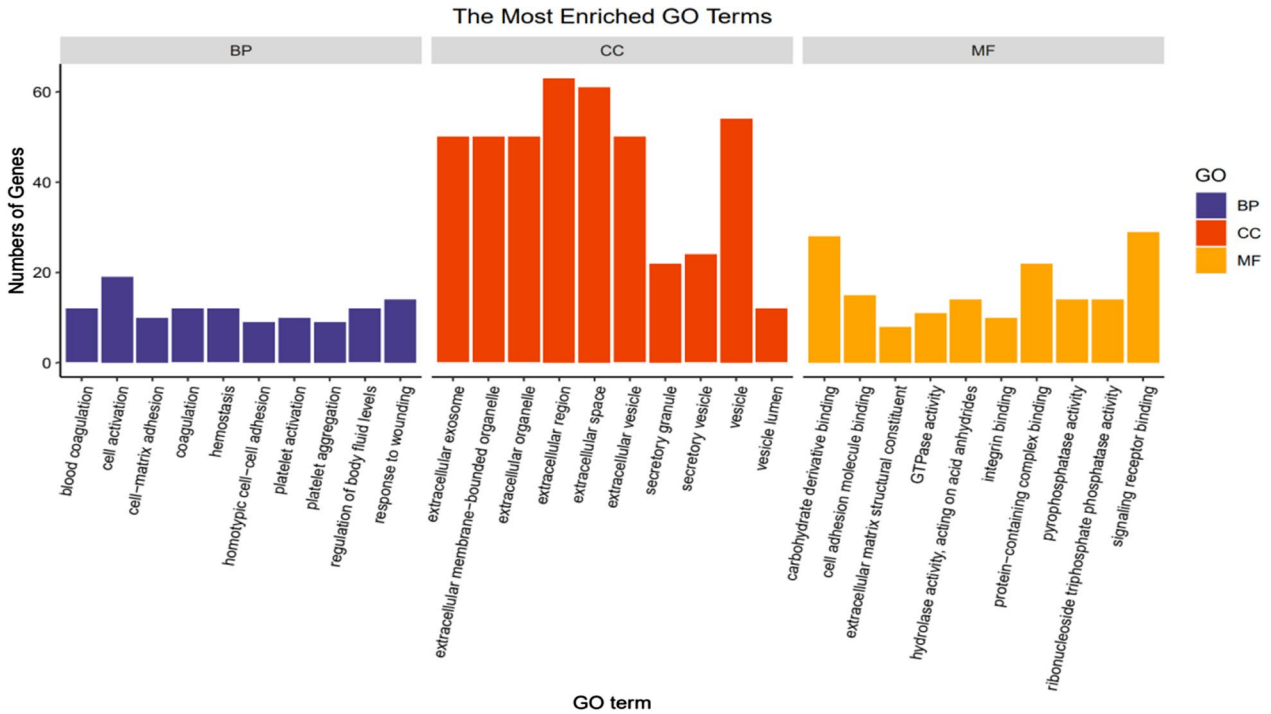

Fig. 3 Differential protein gene ontology (GO) annotation histograms. GO analysis showed that the differentially expressed proteins are involved in biological processes, cellular components, and molecular functions

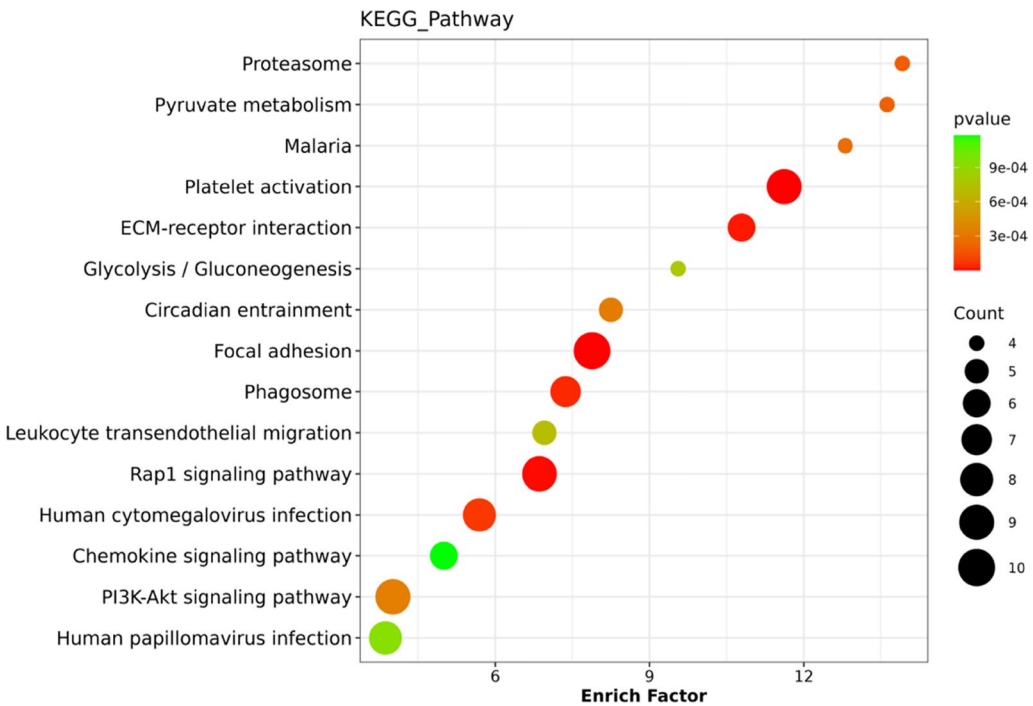

Fig. 4 Distribution bubble map of differentially expressed proteins enriched in Kyoto Encyclopedia of Genes and Genomes (KEGG) pathway categories KEGG analysis showed that the differentially expressed proteins were clustered in multiple pathways

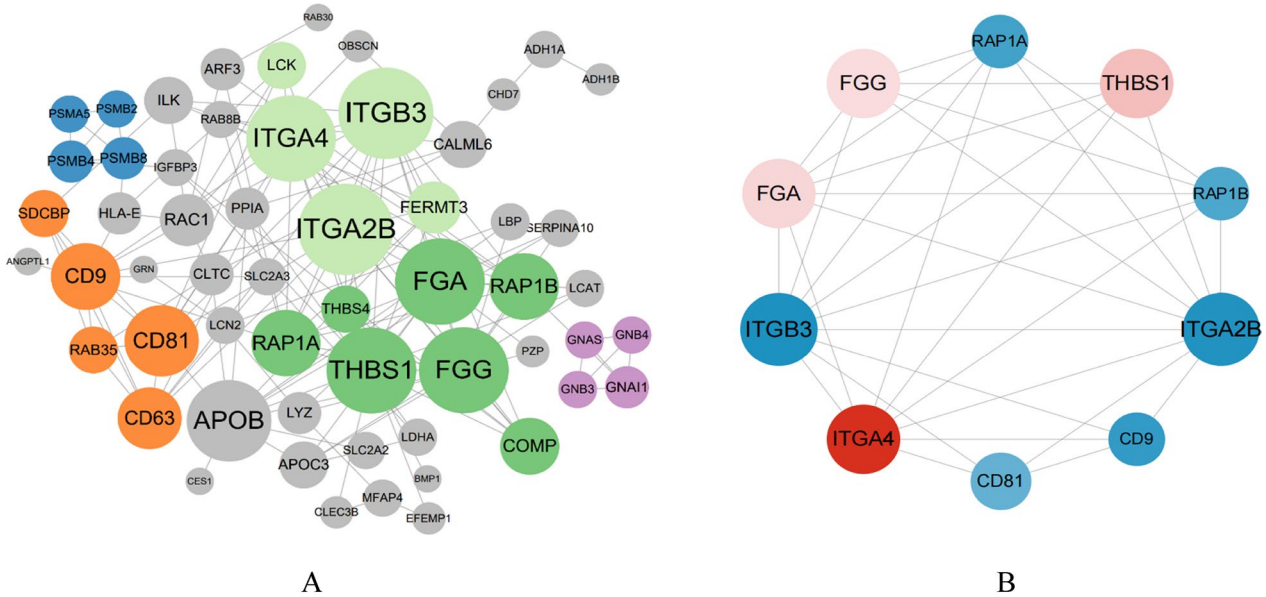

Fig. 5 Analysis of mCRC group and CRC group protein–protein interaction map. **A** Protein interactions analyzed. **B** Top 10 key protein interactions analyzed

RAB35, PSMB4, CD81, CD63, GLIPR2, RAP1B, RAB30, and CES1. The results of WB analysis confirmed that exosomal ITGA4 and GNAI1 levels were significantly higher in mCRC patients than in CRC patients and healthy controls, suggesting that these two proteins may be involved in CRC metastasis via exosomes. Some studies have found that CRC patient populations have different protein profiles, suggesting that plasma exosomal proteomics analysis can be used to better understand the development and metastasis of peritoneal carcinomatosis [25].

Previous studies have linked ITGA4 and SFRP2 gene promoter methylation and tumor differentiation to CRC recurrence, highlighted the role of GNAI1 as a hub node in protein interaction networks, and demonstrated the downregulation of GNAI1 in oxaliplatin-resistant CRC cell lines and hepatocellular carcinoma, where it inhibits cancer cell migration and invasion [26–28]. The expression of PSMB8 is significantly reduced during breast cancer metastasis [29] and is considered a key gene in the tumor microenvironment of cutaneous malignant melanoma [30]. Through PPI network analysis, ITGA4, CD81, CD9, ITGB3, FGA, FGG, THBS1, ITGA2B, RAP1A, and RAP1B were identified as the 10 most closely connected proteins in this study. CD81 has been identified as a new transcriptional target of KLF4, and dysregulated KLF4-CD9/CD81-JNK signaling has been associated with the development of liver cancer [31]. Studies have shown that the unique anti-CD81 antibody 5A6 can inhibit metastasis in vivo, as well as invasion and migration in vitro [32]. CD9 acts as a tumor suppressor in various malignant tumors, with high expression of CD9 in tumor cells often negatively correlated with tumor recurrence, particularly in left-sided CRC [33]. Exosomes containing ITGB3 are considered promising liquid biopsy tissue-specific biomarkers for predicting the early onset and metastasis of CRC. Additionally, ITGB3 plays a role in breast cancer bone metastasis through gene expression regulation [34, 35]. FGA is associated with metastatic gastric cancer [36], while FGG shows potential as a marker for the early diagnosis of non-small-cell lung cancer and is directly related to the survival time of patients with this type of cancer [37]. THBS1 exhibits its potential biochemical characteristics and regulatory functions in CRC invasion and metastasis [38]. There is currently almost no literature on ITGA2B, UGGT, and LBP expression in tumors, suggesting that they may be novel metastasis-related biomarkers. As in most other malignant tumors, the metastasis of CRC is a very complicated process that involves multiple signal pathways and various mechanisms [39].

In this study, mCRC-related genes were found to be mainly enriched in 15 KEGG pathways: proteasome, pyruvate metabolism, malaria, platelet activation, ECM–receptor interactions, glycolysis/gluconeogenesis, circadian entrainment, focal adhesion, phagosome, leukocyte transendothelial migration, Rapl signaling pathway, human cytomegalovirus infection, chemokine signaling pathway, PI3K-Akt signaling pathway, and

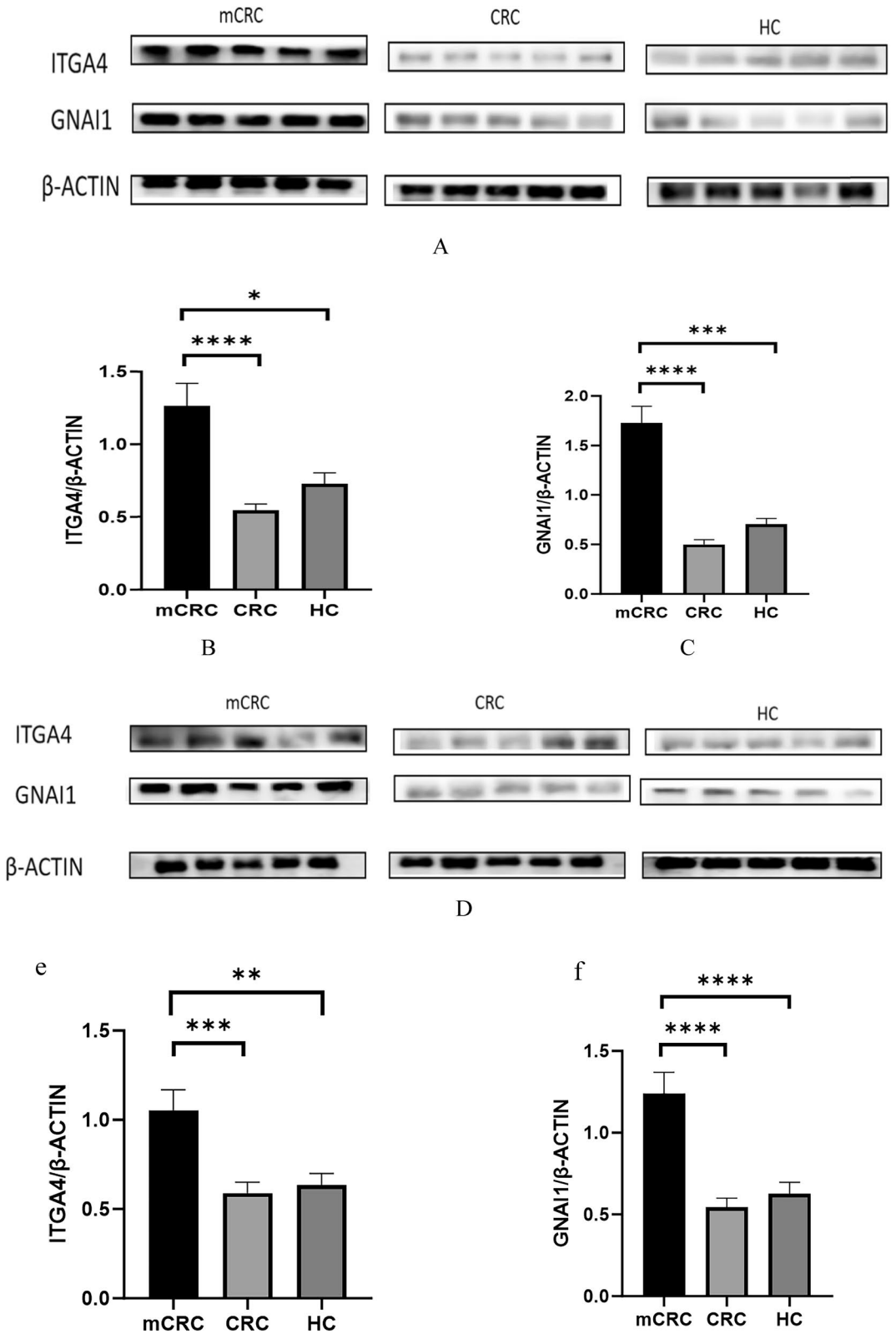

Fig. 6 Validation of exosomal ITGA4 and GNAI1 in individual samples. **A** Western blot analysis of ITGA4 and GNAI1 in exosome samples from mCRC patients, CRC patients, and healthy controls. β-actin was used as an internal control to allow a comparison of equivalent amounts of protein. The corresponding quantified data are shown in **B**, **C**. **D** Western blot analysis of ITGA4 and GNAI1 in exosome samples from five mCRC patients, five CRC patients, and five healthy controls. The corresponding quantified data are shown in **E**, **F**. *$p < 0.05$, **$p < 0.01$, ***$p < 0.001$, ****$p < 0.0001$

human papillomavirus infection. However, more research is warranted to elucidate the mechanisms by which exosomal proteins contribute to mCRC.

However, the extraction of exosomes from a large number of samples may require a more convenient method or the combination of multiple methods. The sample size in this study was relatively small. Although some new plasma exosome proteins related to mCRC were discovered, these need to be verified with a larger sample size, as currently their diagnostic value for mCRC has not been evaluated. The study utilized label-free quantitative proteomics methods to identify mCRC-related differential proteins that could serve as plasma exosome tumor markers. Additional studies using a larger patient cohort are warranted to confirm these findings.

Supplementary Information

The online version contains supplementary material available at https://doi.org/10.1186/s12014-024-09510-8.

Supplementary Material 1.
Supplementary Material 2.
Supplementary Material 3.
Supplementary Material 4.
Supplementary Material 5.
Supplementary Material 6.
Supplementary Material 7.
Supplementary Material 8.
Supplementary Material 9.
Supplementary Material 10.
Supplementary Material 11.
Supplementary Material 12.
Supplementary Material 13.
Supplementary Material 14.
Supplementary Material 15.
Supplementary Material 16.
Supplementary Material 17.
Supplementary Material 18.
Supplementary Material 19.
Supplementary Material 20.
Supplementary Material 21.
Supplementary Material 22.
Supplementary Material 23.

Author contributions

All authors reviewed the manuscript.

Funding

This study was supported by the Science and Technology Project of Karamay Central Hospital of China (YK2022-7).

Data availability

No datasets were generated or analysed during the current study.

Declarations

Ethics approval and consent to participate

The data used in this study have been ethically approved and informed consent has been obtained from the participants in the original research.

Consent for publication

Not applicable.

Competing interests

The authors declare that they have no competing interests.

Received: 18 June 2024 Accepted: 24 September 2024
Published online: 09 October 2024

References

1. Bray F, Ferlay J, Soerjomataram I, et al. Global cancer statistics 2018: GLOBOCAN estimates of incidence and mortality worldwide for 36 cancers in 185 countries. CA Cancer J Clin. 2018;68(6):394–424. https://doi.org/10.3322/caac.21492.
2. Zheng RS, Chen R, Han BF, et al. Cancer incidence and mortality in China, 2022. Zhonghua Zhong Liu Za Zhi. 2024;46(3):221–31. https://doi.org/10.3760/cma.j.cn112152-20240119-00035.
3. Siegel RL, Miller KD, Fuchs HE, et al. Cancer statistics, 2021. CA Cancer J Clin. 2021;71(1):7–33. https://doi.org/10.3322/caac.21654.
4. Shin AE, Giancotti FG, Rustgi AK. Metastatic colorectal cancer: mechanisms and emerging therapeutics. Trends Pharmacol Sci. 2023;44(4):222–36. https://doi.org/10.1016/j.tips.2023.01.003.
5. Sb KIM. Function and therapeutic development of exosomes for cancer therapy. Arch Pharm Res. 2022;45(5):295–308. https://doi.org/10.1007/s12272-022-01387-1.
6. Szajnik M, Derbis M, Lach M, et al. Exosomes in plasma of patients with ovarian carcinoma: potential biomarkers of tumor progression and response to therapy. Gynecol Obstet (Sunnyvale). 2013. https://doi.org/10.4172/2161-0932.S4-003.
7. Wang B, Wei Y, Yang Y, et al. Progress of exosome-related factors in colorectal cancer diagnosis and treatment. China Cancer Clin. 2023;50(12):643–8. https://doi.org/10.12354/j.issn.1000-8179.2023.20230193.
8. Zhao S, Mi Y, Guan B, et al. Tumor-derived exosomal miR-934 induces macrophage M2 polarization to promote liver metastasis of colorectal cancer. J Hematol Oncol. 2020;13(1):156. https://doi.org/10.1186/s13045-020-00991-2.
9. Zheng R, Zhang K, Tan S, et al. Exosomal circLPAR1 functions in colorectal cancer diagnosis and tumorigenesis through suppressing BRD4 via METTL3-eIF3h interaction. Mol Cancer. 2022;21(1):49. https://doi.org/10.1186/s12943-021-01471-y.
10. Wang X, Huang J, Chen W, et al. The updated role of exosomal proteins in the diagnosis, prognosis, and treatment of cancer. Exp Mol Med. 2022;54(9):1390–400. https://doi.org/10.1038/s12276-022-00855-4.
11. Li C, Sun YD, Yu GY, et al. Integrated omics of metastatic colorectal cancer. Cancer Cell. 2020;38(5):734-47.e9.
12. Moon PG, Lee JE, Cho YE, et al. Fibronectin on circulating extracellular vesicles as a liquid biopsy to detect breast cancer. Oncotarget. 2016;7(26):40189–99. https://doi.org/10.18632/oncotarget.9561.
13. Clark DJ, Fondrie WE, Yang A, et al. Triple SILAC quantitative proteomic analysis reveals differential abundance of cell signaling proteins between normal and lung cancer-derived exosomes. J Proteomics. 2016;133:161–9. https://doi.org/10.1016/j.jprot.2015.12.023.
14. Fu Q, Zhang Q, Lou Y, et al. Primary tumor-derived exosomes facilitate metastasis by regulating adhesion of circulating tumor cells via SMAD3 in liver cancer. Oncogene. 2018;37(47):6105–18. https://doi.org/10.1038/s41388-018-0391-0.

15. Umwali Y, Yue CB, Gabriel ANA, et al. Roles of exosomes in diagnosis and treatment of colorectal cancer. World J Clin Cases. 2021;9(18):4467–79. https://doi.org/10.12998/wjcc.v9.i18.4467.
16. Zhou H, Zhu L, Song J, et al. Liquid biopsy at the frontier of detection, prognosis and progression monitoring in colorectal cancer. Mol Cancer. 2022;21(1):86. https://doi.org/10.1186/s12943-022-01556-2.
17. Ma L, Yu H, Zhu Y, et al. Isolation and proteomic profiling of urinary exosomes from patients with colorectal cancer. Proteome Sci. 2023;21(1):3. https://doi.org/10.1186/s12953-023-00203-y.
18. Fu H, Yang H, Zhang X, et al. Exosomal TRIM3 is a novel marker and therapy target for gastric cancer. J Exp Clin Cancer Res. 2018;37(1):162. https://doi.org/10.1186/s13046-018-0825-0.
19. Martins VR, Dias MS, Hainaut P. Tumor-cell-derived microvesicles as carriers of molecular information in cancer. Curr Opin Oncol. 2013;25(1):66–75. https://doi.org/10.1097/CCO.0b013e32835b7c81.
20. Dzunic M, Petkovic I, Cvetanovic A, et al. Current and future targets and therapies in metastatic colorectal cancer. J Buon. 2019;24(5):1785–92.
21. Hoshino A, Kim HS, Bojmar L, et al. Extracellular vesicle and particle biomarkers define multiple human cancers. Cell. 2020;182(4):1044-61.e18. https://doi.org/10.1016/j.cell.2020.07.009.
22. Pan Z, Zheng J, Zhang J, et al. A novel protein encoded by exosomal CircATG4B induces oxaliplatin resistance in colorectal cancer by promoting autophagy. Adv Sci (Weinh). 2022;9(35): e2204513. https://doi.org/10.1002/advs.202204513.
23. Liu W, Yang D, Chen L, et al. Plasma exosomal miRNA-139-3p is a novel biomarker of colorectal cancer. J Cancer. 2020;11(16):4899–906. https://doi.org/10.7150/jca.45548.
24. Zheng R, Matzinger M, Mayer RL, et al. A high-sensitivity low-nanoflow LC–MS configuration for high-throughput sample-limited proteomics. Anal Chem. 2023;95(51):18673–8. https://doi.org/10.1021/acs.analchem.3c03058.
25. Vallejos PA, Fuller RN, Kabagwira J, et al. Exosomal proteins as a source of biomarkers in colon cancer-derived peritoneal carcinomatosis—a pilot study. Proteomics Clin Appl. 2023;17(2): e2100085. https://doi.org/10.1002/prca.202100085.
26. Hong JIN, Liying PANG, Huayang LI, et al. The value of combined detection of ITGA4 and SFRP2 gene methylation in stool in the diagnosis and prognosis of colorectal tumours. J Southern Med Univ. 2021;41(06):891–7. https://doi.org/10.12122/j.issn.1673-4254.2021.06.12.
27. Jianbo XU, Xingyu ZHOU, Qinqin XIE, et al. Bioinformatics analysis and significance of key oxaliplatin resistance genes in colorectal cancer. Chinese Literat Gen Surg (Electron Edn). 2020;14(05):349–54. https://doi.org/10.3877/cma.j.issn.1674-0793.2020.05.007.
28. Yao J, Liang L-H, Zhang Y, et al. GNAI1 suppresses tumor cell migration and invasion and is post-transcriptionally regulated by Mir-320a/c/d in hepatocellular carcinoma. Cancer Biol Med. 2012;9(04):234–41. https://doi.org/10.7497/j.issn.2095-3941.2012.04.003.
29. Szekely B, Bossuyt V, Li X, et al. Immunological differences between primary and metastatic breast cancer. Ann Oncol. 2018;29(11):2232–9. https://doi.org/10.1093/annonc/mdy399.
30. Yan L, Yu Z, Wang H, et al. Bioinformatics analysis identifies PSMB8 as a key gene in the cutaneous malignant melanoma tumor microenvironment. Ann Transl Med. 2022;10(24):1354. https://doi.org/10.21037/atm-22-5761.
31. Li Y, Yu S, Li L, et al. KLF4-mediated upregulation of CD9 and CD81 suppresses hepatocellular carcinoma development via JNK signaling. Cell Death Dis. 2020;11(4):299. https://doi.org/10.1038/s41419-020-2479-z.
32. Abu-Saleh N, Kuo CC, Jiang W, et al. The molecular mechanism of CD81 antibody inhibition of metastasis. Proc Natl Acad Sci USA. 2023;120(26):e2305042120. https://doi.org/10.1073/pnas.2305042120.
33. Kim KJ, Kwon HJ, Kim MC, et al. CD9 expression in colorectal carcinomas and its prognostic significance. J Pathol Transl Med. 2016;50(6):459–68. https://doi.org/10.4132/jptm.2016.10.02.
34. Kovacheva M, Zepp M, Berger S, et al. Conditional knockdown of integrin beta-3 reveals its involvement in osteolytic and soft tissue lesions of breast cancer skeletal metastasis. J Cancer Res Clin Oncol. 2021;147(2):361–71. https://doi.org/10.1007/s00432-020-03428-y.
35. Guo W, Cai Y, Liu X, et al. Single-exosome profiling identifies ITGB3+ and ITGAM+ exosome subpopulations as promising early diagnostic biomarkers and therapeutic targets for colorectal cancer. Research (Wash DC). 2023;6:0041. https://doi.org/10.34133/research.0041.
36. Ding XQ, Wang ZY, Xia D, et al. Proteomic profiling of serum exosomes from patients with metastatic gastric cancer. Front Oncol. 2020;10:1113. https://doi.org/10.3389/fonc.2020.01113.
37. Luo B, Que Z, Lu X, et al. Identification of exosome protein panels as predictive biomarkers for non-small cell lung cancer. Biol Proced Online. 2023;25(1):29. https://doi.org/10.1186/s12575-023-00223-0.
38. Liu X, Li N, Zhang C, et al. Identification of metastasis-associated exoDEPs in colorectal cancer using label-free proteomics. Transl Oncol. 2022;19:101389. https://doi.org/10.1016/j.tranon.2022.
39. Tang Y, Zhao Y, Song X, et al. Tumor-derived exosomal miRNA-320d as a biomarker for metastatic colorectal cancer. J Clin Lab Anal. 2019;33(9):e23004. https://doi.org/10.1002/jcla.23004.

Publisher's Note